An EPR Study of the Dinuclear Iron Site in the Soluble Methane Monooxygenase from *Methylococcus capsulatus* (Bath) Reduced by One Electron at 77 K: The Effects of Component Interactions and the Binding of Small Molecules to the Diiron(III) Center†

Roman Davydov,‡,§ Ann M. Valentine,§ Sonja Komar-Panicucci,§ Brian M. Hoffman,*,‡ and Stephen J. Lippard*,§

Departments of Chemistry, Northwestern University, Evanston, Illinois 60208, and Massachusetts Institute of Technology, Cambridge, Massachusetts 02139

Received October 6, 1998; Revised Manuscript Received January 20, 1999

ABSTRACT: Reduction of the soluble methane monooxygenase hydroxylase (MMOH) from *Methylococcus capsulatus* (Bath) in frozen 4:1 buffer/glycerol solutions at 77 K by mobile electrons generated by γ-irradiation produces an EPR-detectable, mixed-valent Fe(II)Fe(III) center. At this temperature the conformation of the enzyme remains essentially unaltered during reduction, so the mixed-valent EPR spectra serve to probe the active site structure of the EPR-silent, diiron(III) state. The EPR spectra of the cryoreduced samples reveal that the diiron(III) cluster of the resting hydroxylase has at least two chemically distinct forms, the structures of which differ from that of the equilibrium Fe(II)Fe(III) site. Their relative populations depend on pH, the presence of component B, and formation of the MMOH/MMOB complex by reoxidation of the reduced, diiron(II) hydroxylase. The formation of complexes between MMOB, MMOR, and the oxidized hydroxylase does not measurably affect the structure of the diiron(III) site. Cryogenic reduction in combination with EPR spectroscopy has also provided information about interaction of MMOH in the diiron(III) state with small molecules. The diiron(III) center binds methanol and phenols, whereas DMSO and methane have no measurable effect on the EPR properties of cryoreduced hydroxylase. Addition of component B favors the binding of some exogenous ligands, such as DMSO and glycerol, to the active site diiron(III) state and markedly perturbs the structure of the diiron(III) cluster complexed with methanol or phenol. The results reveal different reactivity of the Fe(III)Fe(III) and Fe(II)Fe(III) redox states of MMOH toward exogenous ligands. Moreover, unlike oxidized hydroxylase, the binding of exogenous ligands to the protein in the mixed-valent state is allosterically inhibited by MMOB. The differential reactivity of the hydroxylase in its diiron(III) and mixed-valent states toward small molecules, as well as the structural basis for the regulatory effects of component B, is interpreted in terms of a model involving carboxylate shifts of a flexible glutamate ligand at the Fe(II)Fe(III) center.

The methanotrophic bacterium *Methylococcus capsulatus* (Bath) can express a soluble, multicomponent enzyme system, methane monooxygenase or sMMO,[1] responsible for the NADH- and dioxygen-dependent hydroxylation of methane to methanol (*1*−*3*). Substrate binding and O_2 activation occur at non-heme diiron catalytic sites located in the α subunits of the 251 kDa hydroxylase component, MMOH, an $\alpha_2\beta_2\gamma_2$ homodimer. A 15.8 kDa monomeric protein termed component B, MMOB, couples hydrocarbon oxidation in MMOH with the transfer of electrons from the NADH-reduced form of MMOR, the 38.5 kDa reductase component (*4, 5*). Kinetic and potentiometric studies indicate that interactions with MMOR and MMOB affect the electron transfer and redox properties, oxygenase activity, and electronic structure of the dinuclear iron sites in MMOH (*3, 4, 6*). Spectroscopic experiments further reveal that binding of MMOB as well as small exogenous molecules can alter the properties of the active site diiron clusters in their mixed-valent and fully reduced states. In particular, the electron paramagnetic resonance (EPR) spectrum of the mixed-valent form of MMOH is significantly different in the presence of MMOB or exogenous ligands such as dimethyl sulfoxide (DMSO) or methanol (*7, 8*). A large shift in g_{av} from 1.82 and altered power saturation behavior are both observed (*7, 9*). Also, CD and MCD studies reveal that the binding of MMOB and some substrates and inhibitors perturbs the diiron(II) clusters in the reduced hydroxylase component

† This work was supported by Grants GM32134 (to S.J.L.) and HL13531 (to B.M.H.) from the NIH and NSF Grant MCB 9507061 (to B.M.H.). S. K.-P. was supported by a postdoctoral fellowship from NIGMS.

* To whom correspondence should be addressed.

‡ Northwestern University.

§ Massachusetts Institute of Technology.

[1] Abbreviations: sMMO, soluble methane monooxygenase; MMOH, methane monooxygenase hydroxylase; MMOB, methane monooxygenase component B; MMOR, methane monooxygenase reductase; EPR, electron paramagnetic resonance; ENDOR, electron nuclear double resonance; DMSO, dimethyl sulfoxide; CD, circular dichroism; MCD, magnetic circular dichroism; RNR, ribonucleotide reductase; Hr, hemerythrin; H_{ox}, oxidized MMOH; H_{mv}, mixed-valent (Fe^{III}, Fe^{II}) MMOH prepared by chemical reduction at room temperature; Hox_{mv}, mixed-valent MMOH retaining H_{ox} structure prepared by radiolytic reduction at 77 K.

10.1021/bi982391o CCC: $18.00
Published on Web 03/09/1999

from *Methylosinus trichosporium* OB3b (*10*).

The three-dimensional structures of the resting, oxidized state of MMOH from *M. capsulatus* (Bath) (*11*, *12*) and from *M. trichosporium* OB3b (*13*) have been determined. The iron atoms in the *M. capsulatus* (Bath) enzyme are bridged by a hydroxide ion and a bidentate, semibridging glutamate ligand. Each metal atom is also coordinated to a histidine ligand. Two additional glutamate residues ligate one iron atom in a monodentate fashion, whereas the other iron atom has a monodentate glutamate and a water molecule in its coordination sphere. Finally, octahedral coordination at each of the iron atoms is completed by an exogenous bridging ligand, assigned either as water in flash frozen (−160 °C) crystals (*12*) or acetate from the crystallization buffer in crystals prepared at 4 °C (*11*). The structure of the diiron core in the hydroxylase from *M. trichosporium* OB3b crystallized at 18 °C is very similar to that in flash frozen crystals of MMOH from *M. capsulatus* (Bath) (*13*). In the reduced diiron(II) form of the latter enzyme, the metal atoms are no longer bridged by exogenous OH^- and H_2O ligands but by the oxygen atom of glutamate coordinated in a μ-η^2 fashion (*12*, *14*). Structural diagrams of the diiron cores of oxidized and reduced MMOH from *M. capsulatus* (Bath) are presented in Figure 1.

Although the effects of MMOB and small molecule binding to the mixed-valent and diiron(II) states of MMOH have been studied, very little information is available concerning the structural consequences of MMOB and substrate/inhibitor interactions with the resting, diiron(III) MMOH. Studies using Mössbauer (*9*, *15*) and EXAFS spectroscopy (*16*, *17*) have failed to detect any significant alterations in the diiron cluster that could be associated with the dramatic effects of MMOB, reductase, and substrate on catalysis.

Previously the EPR spectra of dinuclear clusters in the R2 protein of ribonucleotide reductase (R2 of RNR), hemerythrin (Hr), and MMOH from *M. trichosporium* OB3b, reduced by one electron in frozen solutions, proved to be structurally sensitive probes for the EPR-silent diiron(III) states of these proteins (*18*−*21*). In these studies, the bridged diiron(III) sites of the proteins at 77 K were reduced by mobile electrons generated by γ-irradiation. The mixed-valent diiron cluster trapped in this fashion retains a conformation close to that of the original diiron(III) form because it cannot relax to an equilibrium state in the solid matrix (*18*−*21*). The conformation of the mixed-valent hydroxylase so constrained will be in a nonequilibrium state if the coordination environment of the diiron cluster depends on the redox level of the iron atom(s). The mixed-valent species in such a nonequilibrium state can relax to the corresponding equilibrium state at higher temperatures, 160−270 K for the R2 protein of RNR, Hr, and MMOH (*18*−*21*). The EPR spectra of species obtained by such an annealing process are identical to those obtained following chemical reduction in fluid solution.

Application of this approach to MMOH from *M. trichosporium* OB3b revealed the presence of two different conformers in the resting, diiron(III) state, the structures of which differed from that of the mixed-valent enzyme (*20*). Moreover, MMOB had an effect on the diiron site of oxidized MMOH which was different than that previously observed for the mixed-valent form. In the present work we have used

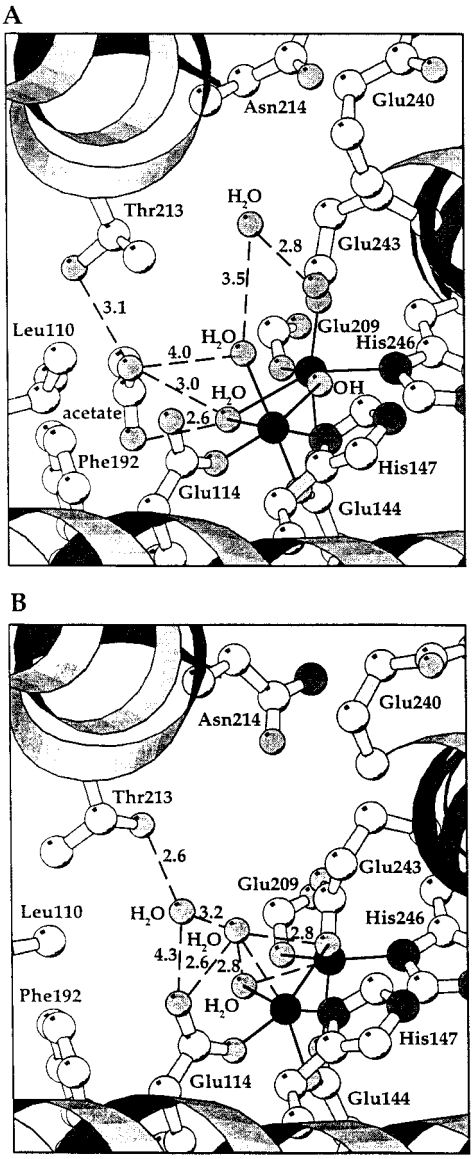

FIGURE 1: The diiron active site of MMOH in the oxidized diiron(III) (A) and reduced diiron(II) (B) states (*12*). Hydrogen bonding interactions are depicted along dashed lines, with the distances indicated. Fe and N atoms are represented as solid spheres.

the low-temperature reduction methodology to probe the diiron(III) center in the oxidized hydroxylase component from *M. capsulatus* (Bath), examining the effects of component B and MMOR on the active site. We have studied the interaction of substrate, product, and several other small molecules with oxidized hydroxylase and the effects of component B on this interaction. The results provide insights into the reactivity of the oxidized and mixed-valent forms of the hydroxylase as well as the structural basis for the regulatory effects of component B.

MATERIALS AND METHODS

MMOH and MMOR from *M. capsulatus* (Bath) and recombinant protein B were isolated, purified, and characterized as previously described (*9*, *22*, *23*). All reagents including D_2O (99.9% D; Cambridge Isotope Labs) were obtained from commercial sources and used as received. Unless otherwise specified, protein samples were prepared in buffer, 25 mM MOPS (pH 7.0)/glycerol, 4:1 by volume.

H_2O was exchanged into D_2O to reduce the intensity of free radical signals induced in the matrix by γ-radiolysis which partly overlap with the mixed-valent diiron signal. The final concentration of hydroxylase in the samples was 0.65−0.90 mM. For hydroxylase samples prepared with MMOB present, the MMOB/MMOH ratio was 2:1. A ternary mixture MMOH/MMOB/MMOR was prepared by adding a stoichiometric amount of reductase to the preformed 1:2 complex of H_{ox} with MMOB. Typically 2 vol % of dimethyl sulfoxide (DMSO) or methanol (MeOH), or 25−50 mM phenol was added to sMMO in studies with these reagents present.

Protein samples were chemically reduced to the mixed-valent state according to a previously reported method (*8*). Reoxidized protein was prepared from diiron(II) MMOH in the presence of two equivalents of MMOB by reduction according to a published procedure (*6*) followed by rapid reoxidation in air with gentle agitation and freezing to 77 K within two minutes. Oxidized protein samples were frozen in liquid nitrogen in 3 mm i.d. EPR quartz tubes and exposed to γ-irradiation from a ^{60}Co source at a dose rate of 0.46 Mrad h^{-1} for a time sufficient to achieve a total dose of 2.7−3.2 Mrad.

X-band EPR spectra were recorded on Bruker ESP300 or EMX spectrometers equipped with an Oxford Instrument ESR900 liquid helium cryostat. The field modulation was set at 100 kHz. The spin concentration of the mixed-valent signal was quantitated under nonsaturating conditions by using a standard 1 mM Cu(II)/EDTA solution (*18*). EPR spectra at 35 GHz were recorded at 2 K in the rapid-passage dispersion mode on a locally constructed instrument described elsewhere (*24*).

Annealing of cryogenically reduced samples was performed in cooled isopentane for the given time at the stated temperature. Samples were then rapidly cooled to 77 K.

RESULTS

One-Electron Cryogenic Reduction of Hydroxylase. Figure 2 presents the low-temperature X-band EPR spectra of MMOH in the mixed-valent state generated either by chemical reduction at room temperature (H_{mv}) (Figure 2A) or by radiolytic reduction at 77 K (Hox_{mv}) (Figure 2B−C). H_{mv} exhibits a rhombic signal with g values of 1.94, 1.87, and 1.72, similar to that reported previously (*8*). Table 1 lists the g values for all species discussed in this article. Cryogenically reduced H_{ox} exhibits a more complex $g < 2$ EPR spectrum (Figure 2B), the shape of which is nearly independent of irradiation dose in the 0.8−3.8 Mrad range. Quantitation of the mixed-valent spectrum in Figure 2B under nonsaturating conditions indicates that the total yield of a paramagnetic, $S = {}^1/_2$ species upon cryogenic reduction of H_{ox} is 25% ± 5% of the diiron centers at a dose of 2.7 Mrad. This spectrum varies only slightly with the glycerol content of the sample in the 15−50% range (data not shown).

The spectrum of Hox_{mv} is broadened above 15 K and its shape depends upon both temperature and applied microwave power below 6 K (Figure 2C). In the temperature range between 7 and 15 K, a rhombic mixed-valent pattern with g values of 1.94, 1.86, and 1.79 ($g_{av} = 1.85$, designated H1) dominates, but additional high-field resonances belonging to a signal designated H2 are also observed (Figure 2B). Q-band EPR spectra (not shown) indicate that the H1 signal

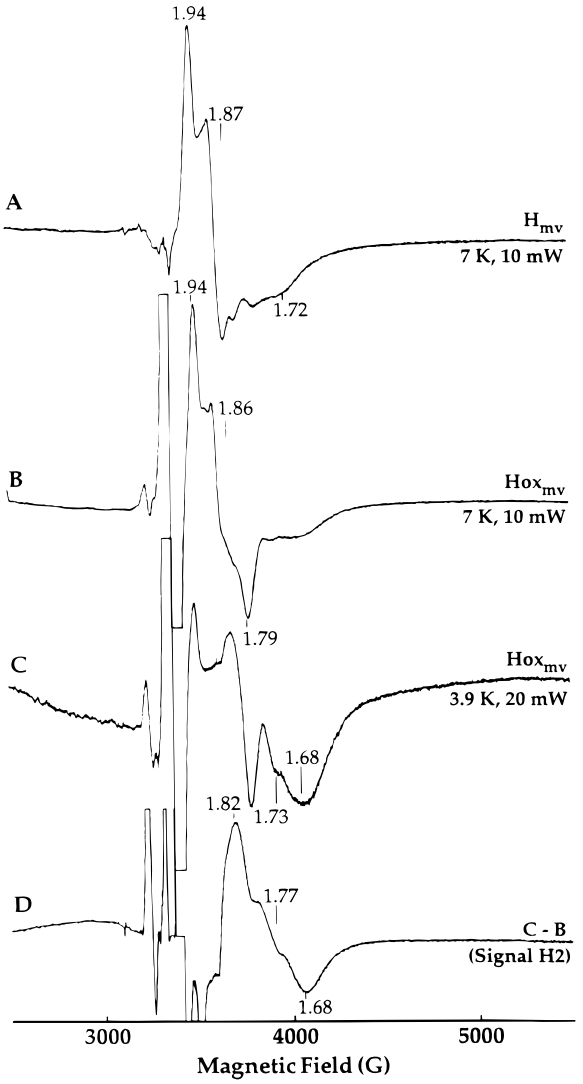

FIGURE 2: X-band EPR spectra of mixed-valent forms of MMOH (pH 7.0) generated chemically at room temperature (A) and in 4:1 buffer/glycerol generated radiolytically at 77 K (B, C); (D) difference spectrum of the signal H2 obtained by subtraction of scaled spectrum B from spectrum C as described in text. Instrument parameters: modulation frequency, 100 kHz; modulation amplitude, 10 G; gain, 5000; and frequency, 9.235. (A) 7 K, 10 mW; (B) 7 K, 10 mW; (C) 3.9 K, 20 mW.

itself represents a set of very similar species. The intensities of the H2 features increase markedly at 3.9 K (Figure 2C) as applied microwave power is increased up to 70 mW, and the H2 signal may be obtained by subtraction of the scaled H1 signal. The difference spectrum presented in Figure 2D reveals the resulting signal of H2, which has effective g values of 1.82, 1.77, and 1.68 (g_{av} 1.74)**.** Because cryogenic reduction retains a "footprint" of the diiron(III) geometry, the occurrence of two different signals indicates that H_{ox} exists in two chemically or conformationally distinct forms. We estimate that the H2 form is less than 20% of the total mixed-valent species generated, but accurate quantitation is not possible.

Spectra of Hox_{mv} depend slightly on pH in the 6.1−8.2 range (Figure S1 in Supporting Information). Reducing the pH to 6.1 results in a slight modification of the shape of signal H2 (Figure S1A). At pH 8.2, the $g_2 = 1.86$ component of H1 becomes slightly broadened and the relative intensity

Table 1: Effective *g* Values for Mixed-Valent Species of MMOH Produced by Reduction at 77 or 293 K

mixed-valent species of hydroxylase	signal	effective ***g*** values
H_{mv}		1.94, 1.87, 1.72
Hox_{mv}	H1	1.94, 1.86, 1.79
	H2	1.82, 1.77, 1.68
H_{mv} + MeOH		1.94, 1.86, 1.69
$(H_{ox}$ + MeOH$)_{mv}$	H1M	1.95, 1.87, 1.75
	H2M	1.84, 1.74, 1.60
H_{mv} + *p*-NO_2Ph		1.95, 1.86, 1.75
$(H_{ox}$ + *p*-NO_2Ph$)_{mv}$	H1Pa	1.95, 1.80, 1.80
	H1Pb	1.94, 1.87, 1.81
H_{mv} + DMSO		1.95, 1.85, 1.80
$(H_{ox}$ + DMSO$)_{mv}$	H1	1.94, 1.86, 1.79
	H2	1.82, 1.77, 1.68
H_{mv} + MMOB	HB1	1.88, 1.77, 1.63
$(H_{ox}$ + MMOB$)_{mv}$	H1	1.94, 1.86, 1.79
	H2	1.82, 1.77, 1.68
$(H_{ox}$ + MMOB + MeOH$)_{mv}$		1.95, 1.86, 1.74
$(H_{ox}$ + MMOB + glycerol$)_{mv}$	HB2	1.90, 1.87, 1.83

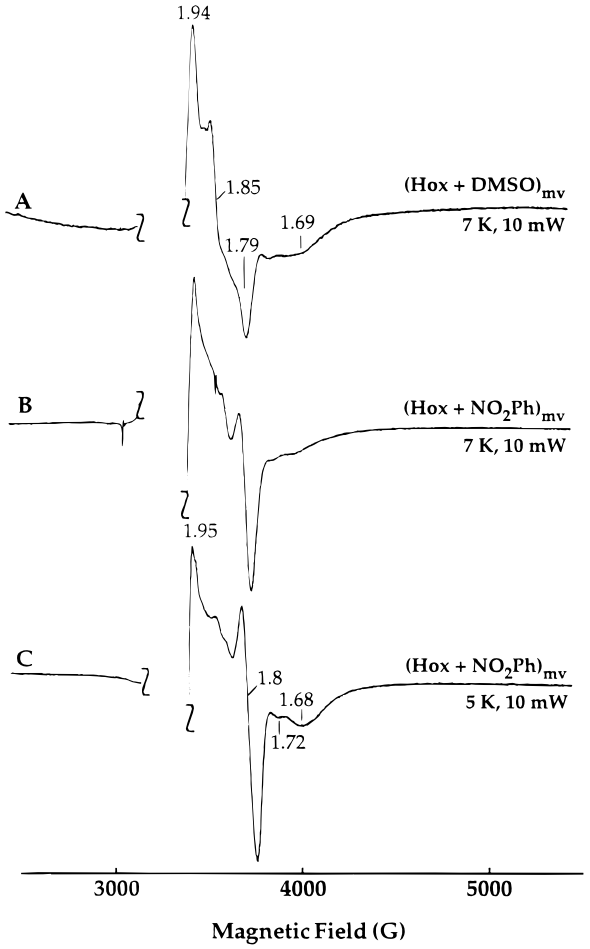

FIGURE 3: X-band EPR spectra of oxidized hydroxylase in the presence of 0.25 M DMSO (A) and 50 mM *p*-nitrophenol (B, C) radiolytically reduced at 77 K. In this and the remaining figures, the offscale $g = 2$ signal due to radical species generated by radiolytic reduction (see Figure 2A−C) is truncated for clarity. Instrument conditions were as in Figure 2 except for (A) 7 K, 10 mW; (B) 7 K, 10 mW; and (C) 5 K, 10 mW.

of the H2 component decreases so that the ratio of the populations H1 and H2 becomes roughly 9:1 (Figure S1B).

Effect of Small Molecules on Hox_{mv}. The EPR spectrum of H_{mv} is sensitive to exogenous ligands such as dimethyl sulfoxide (*8*, *23*) and methanol (*14*, *23*, *24*) (see also Figures

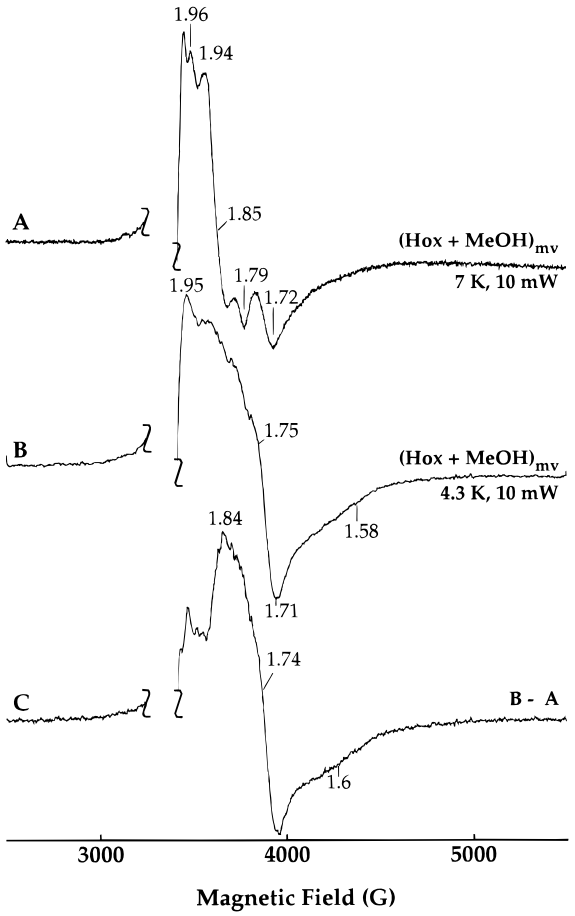

FIGURE 4: X-band EPR spectra of mixed-valent form of MMOH in the presence of 2% methanol produced by reduction at 77 K (A, B); (C) difference spectrum (B − A). Instrument parameters were as in Figure 2 except for (A) 7 K, 10 mW; and (B) 4.3 K, 10 mW.

S2, S3). Addition of phenol, *p*-nitrophenol, or *p*-fluorophenol also significantly perturbs the EPR spectrum of H_{mv} (Figure S4). In the presence of 50 mM phenol, the g_{eff} values shift to 1.94, 1.88, and 1.82 (phenol), 1.95, 1.86, and 1.75 (*p*-nitrophenol), and 1.94, 1.86, and 1.78 (*p*-fluorophenol), respectively.

Unlike the major spectral changes that occur when DMSO is added to H_{mv} produced at room temperature, EPR spectra of Hox_{mv} generated at 77 K in the presence (Figure 3A) or absence (Figure 2B) of 0.25 M DMSO are indistinguishable. This result indicates that DMSO probably does not bind to the diiron(III) cluster.

By contrast, *p*-nitrophenol and methanol cause dramatic changes in the EPR spectrum of Hox_{mv}, as shown in Figures 3B,C and 4. This result suggests that these exogenous agents bind to the diiron(III) cluster. There is prior spectroscopic evidence, formation of a purple color assigned as a ligand-to-metal charge-transfer band, for direct binding of phenol to the diiron cluster of H_{ox} from *M. trichosporium* OB3b (*25*), although no such feature has yet been detected for the *M. capsulatus* (Bath) enzyme. In the EPR spectra of (H_{ox} + *p*-nitrophenol)$_{mv}$ (Figure 3B,C), signal H2 remains practically unchanged whereas signal H1 disappears and at least two new EPR signals, designated H1Pa and H1Pb, can be identified from their different temperature-dependent relaxation behavior. At 5 K and below (Figure 3C), an axial signal H1Pa having $g_{||} = 1.95$ and $g_{\perp} = 1.80$ is clearly seen, whereas

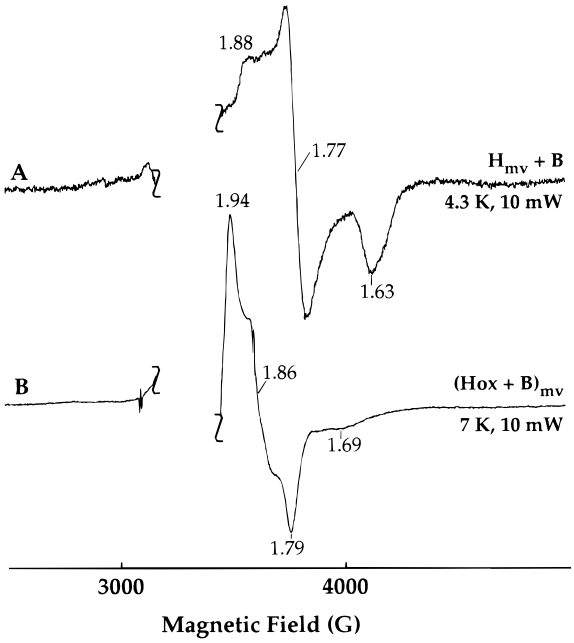

FIGURE 5: X-band EPR spectra of mixed-valent forms of the hydroxylase + component B complex produced by chemical reduction at room temperature (A) and by radiolytic reduction at 77 K (B). Instrument conditions were as in Figure 2 except for (A) 4.3K, 10 mW; and (B) 7K, 10 mW.

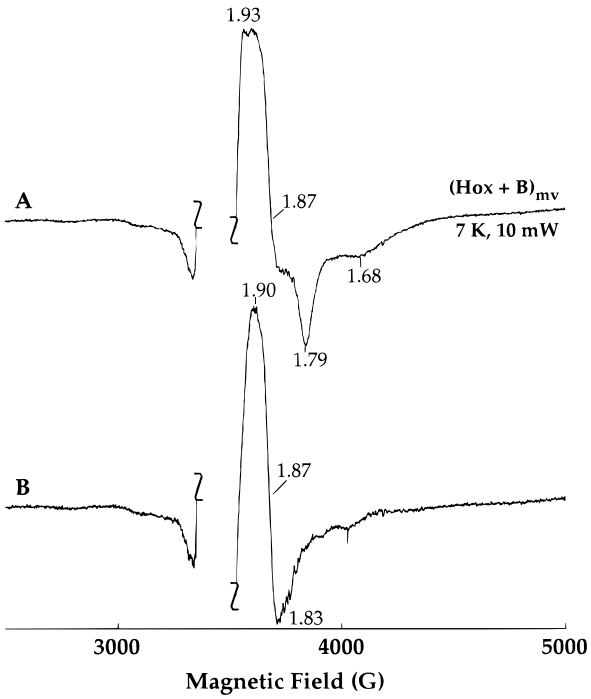

FIGURE 6: X-band EPR spectra of the H_{ox} + MMOB complex in 1:1 buffer/glycerol one-electron-reduced at 77 K (A); (B) difference spectrum of signal HB2 obtained by subtraction of the spectrum of Figure 2B from spectrum A. Instrument parameters were as in Figure 2 except for (A) 7 K, 10 mW.

at higher temperatures (data not shown) an additional signal(s) H1Pb, slightly different from signal H1 and having g values of 1.94, 1.87, and 1.81, is observed. We conclude that *p*-nitrophenol binds to the diiron(III) cluster of H1Pa and binds at or near the diiron(III) cluster of H1Pb. Either conformer H2 does not interact with the exogenous ligand under the conditions employed or, less likely, its binding in the active site cavity does not noticeably perturb the EPR properties of the mixed-valent state.

The EPR spectra of $(H_{ox} + MeOH)_{mv}$ (Figure 4A,B) comprise at least three distinct EPR signals. The sharp H1 signal from Hox_{mv} is easily distinguished at $T > 9$ K. The main intensities come from two new species (H1M and H2M). The H1M signal can be better resolved in a 35 GHz spectrum and is characterized by $g_{eff} = 1.95$, 1.87, and 1.75 ($g_{av} = 1.86$); signal H2M is observable below 6 K and was detected by subtracting mixed-valent spectra recorded at 4.3 and 7 K (Figure 4C). The dramatic perturbations in the EPR spectra of cryogenically reduced MMOH induced by methanol (compare 4A and C with 2B and D) strongly indicate that MeOH binds to the diiron(III) active site. Furthermore in $(H_{ox} + MeOH)_{mv}$, the relative content of H2M species is increased remarkably relative to that of species H2 in the Hox_{mv} sample, which has comparable g values.

Cryogenic Reduction of the H_{ox} + MMOB Complex in the Presence and Absence of Small Molecules and MMOR. Addition of MMOB to H_{mv} generated at room temperature perturbs the EPR properties of the latter (*7*, *9*, *15*). The (H_{mv} + MMOB) complex affords a broad EPR signal (HB1) with effective g values of 1.88, 1.77, and 1.63 (Figure 5A) that is difficult to detect at 7 K and above. It differs significantly from the EPR spectrum of the $(H_{ox} + MMOB)_{mv}$ generated at 77 K (Figure 5B).[2] MMOB binding does not alter the shape of the Hox_{mv} H2 signal and only slightly perturbs the shape of the $g_2 = 1.86$ component of the Hox_{mv} H1 signal. MMOB does diminish the relative contribution of the H2 signal, however, by a factor of about 1.6 (cf. Figures 5B and 2B). These results reveal that binding of MMOB to the resting hydroxylase changes the relative populations of the two diiron(III) forms, while not perturbing the diiron(III) cluster sufficiently to change the spectroscopic properties of Hox_{mv}. When the (H_{ox} + MMOB) complex is prepared by reoxidation of the fully reduced complex (H_{red} + MMOB) with O_2, the amount of species H2 increases by a factor of 3 compared to $(H_{ox} + MMOB)_{mv}$.

The influence of MMOB on the EPR properties of the diiron cluster in Hox_{mv} is significantly enhanced in the presence of higher glycerol concentrations, although glycerol itself does not perturb the EPR spectrum of Hox_{mv}. In 50% glycerol, a new signal for $(H_{ox} + MMOB)_{mv}$ appears at the expense of H1 and H2 (Figure 6A). This signal, designated HB2 and shown in Figure 6B, is detected by subtracting the EPR spectrum of uncomplexed Hox_{mv} from that of Figure 6A. It is characterized by effective g values of 1.9, 1.87, and 1.83 ($g_{av} = 1.87$). The signal is relatively easily saturated at 7 K, with $P_{1/2} < 2$ mW. The observed effect of MMOB binding on the EPR properties of Hox_{mv} at high concentrations of glycerol may be due to binding of this small molecule at the active site.

Although DMSO has no influence on the EPR spectrum of Hox_{mv}, addition of this reagent has a profound effect on the EPR spectrum of $(H_{ox} + MMOB)_{mv}$ (Figure 7A vs Figure

[2] Mixed-valent species trapped upon cryogenic reduction of $MMOH_{ox}$ + B sometimes include a very small percentage (2−5%) of an unusual, very narrow $S = {}^1/_2$ signal with g values of 1.96, 1.94, and 1.89 observable even at 77 K. Such a narrow spread in g values is characteristic of oxo-bridged Fe(II)Fe(III) cores (*26*).

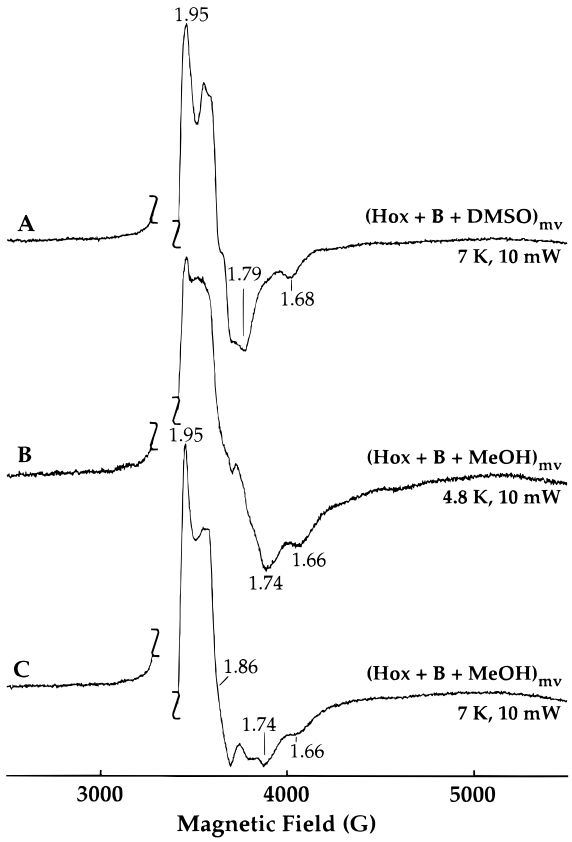

FIGURE 7: X-band EPR spectra of the H_{ox} + MMOB complex in the presence of 2% DMSO (A) and 2% methanol (B, C) radiolytically reduced at 77 K. Instrument parameters were as in Figure 2 except for (A) 7 K, 10 mW; (B) 4.8 K, 10 mW; and (C) 7 K, 10 mW.

5B). Spectra recorded below 5 K reveal the loss of the anisotropic EPR signal from species H2 (data not shown), leaving only signals that are of the H1 type. In addition, the 7 K spectrum (Figure 7A) of these H1-type signals differs from that of $(H_{ox} + MMOB)_{mv}$ in the absence of DMSO (Figure 6B). The similarity in relaxation properties of mixed-valent species in $(H_{ox} + MMOB + DMSO)_{mv}$ makes it difficult to deconvolute unambiguously the spectra into separate EPR signals. Nonetheless, these observations provide evidence that DMSO causes a major change in the relative populations of H1 and H2 diiron clusters, and in some manner MMOB alters the influence of DMSO on the active site H1 diiron(III) centers in H_{ox}.

MMOB binding also perturbs the EPR spectrum of $(H_{ox} + MeOH)_{mv}$. The anisotropic H2M signal completely disappears (Figure 7B), and signal H1M becomes better resolved (Figure 7B,C). In contrast, component B exerts a minor effect on the mixed-valent spectrum of low-temperature reduced, H_{ox} + *p*-nitrophenol complex (data not shown).

Taken together, these results indicate that the EPR spectroscopic properties of the cryogenically reduced diiron cluster, which reflect the diiron(III) active site structure, are sensitive to MMOB binding only when an exogenous agent such as DMSO, glycerol, methanol, or phenol is present.

Annealing of the Samples. Neither methane nor MMOR affects the mixed-valent spectra of the $(H_{ox} + MMOB)_{mv}$ complex (data not shown). Weak but reproducible distinctions between the EPR spectra of cryogenically reduced H_{ox} + MMOB and H_{ox} + MMOB + MMOR ternary mixtures appear only after annealing the samples at 115 K for 15 min, conditions under which significant structural rearrangements or diffusion-controlled intermolecular processes do not occur. Annealing the samples reduces the H1 signal intensity and perturbs the shape and increases the intensity of the H2 signal (data not shown). The spectroscopic distinctions between the annealed samples are manifest mainly as differences in the line shapes of the anisotropic H2 signal (data not shown). Annealing experiments at 115 K in frozen water/glycerol solutions carried out with other carboxylate-bridged diiron proteins and model compounds reduced at 77 K similarly revealed only minor alterations in the EPR spectra attributed to outer sphere perturbations of ligation geometry (*18*−*21*, *26*).

The mixed-valent species of H_{ox} alone, DMSO-, methanol-, or phenol-treated H_{ox}, and the H_{ox} + MMOB complex all relax to their corresponding equilibrium states after annealing the samples at 293 K for 3−7 min (data not shown). The EPR properties of these relaxed forms are nearly indistinguishable from those of the respective mixed-valent forms of MMOH generated at room temperature. It is of particular interest that $(H_{ox} + MMOB + L)_{mv}$, where L = MeOH or phenol, annealed at 293 K exhibit mixed-valent spectra comprising only the EPR signals of H_{mv} + ligand and H_{mv} + MMOB. The spectrum of annealed $(H_{ox} + MMOB + DMSO)_{mv}$ was the same as that of annealed $(H_{ox} + DMSO)_{mv}$, possible reasons for which are discussed below. The transition of the matrix-constrained mixed-valent hydroxylase to the equilibrium state proceeds through several EPR-distinguishable transient intermediates which are differentially stabilized at intermediate temperatures. In particular, upon annealing at 240 K for 3 min, all cryoreduced H_{ox} + MMOB samples displayed a new transient mixed-valent intermediate having a rhombic EPR signal with *g* values centered at 1.836, 1.67, and 1.47 (data not shown). In most cases, however, the samples annealed at temperatures below 240 K revealed several mixed-valent intermediates present simultaneously, making it difficult to identify and analyze unambiguously the EPR component signals.

DISCUSSION

The Nature of Cryoreduced MMOH. Radiolytic reduction of the diiron(III) core at the active site of the MMO hydroxylase enzyme in frozen 4:1 buffer/glycerol solutions at 77 K affords the trapped Fe(II)Fe(III) mixed-valent Hox_{mv} species in 25% ± 5% yield based on iron sites at a dose of 2.7 Mrad. In the absence of MMOB or small molecule additives, the spectrum of MMOH reduced by one electron at 77 K revealed at least two distinct populations of Fe(II)-Fe(III) clusters giving rise to the $g < 2$ EPR signals H1 and H2 (Figure 2B,D). The relative contributions of these species were essentially independent of irradiation dose in the studied range. Mixed-valent intermediates with similar EPR properties were recently reported for MMOH from *M. trichosporium* OB3b radiolytically reduced at 77 K in a frozen 1:1 buffer/glycerol glass (*20*). The spectra for the two enzymes differ only in that the latter enzyme exhibits a more homogeneous H1 EPR signal and a more intense H2 signal. The H1 and H2 signals differ from that of H_{mv} generated at room temperature in both *g* values and relaxation characteristics.

Scheme 1

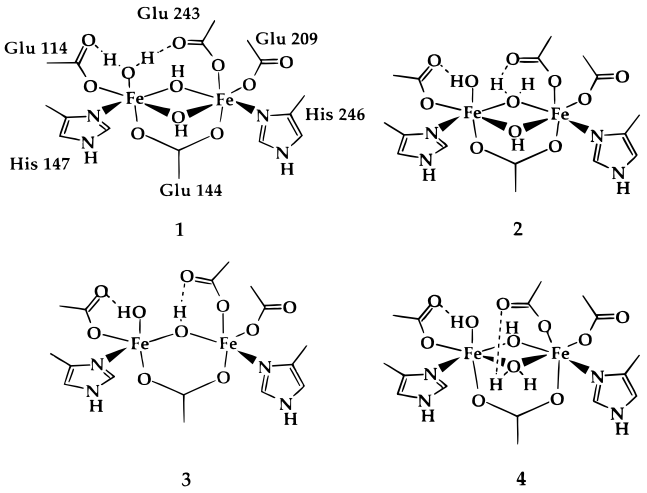

Given that cryogenic reduction preserves the active site diiron(III) cluster geometry, we may draw the following conclusions. The resting oxidized hydroxylase in solution has at least two populations of distinct diiron sites, and their structures are different from that of the Fe(II)Fe(III) center in the equilibrium form of the protein generated at room temperature. The observation of two distinguishable diiron(III) structures for the resting form of the enzyme is not surprising given the variety of oxidized structures exhibiting carboxylate-shifted glutamate residues revealed by X-ray crystallography (*11*−*13*) and the heterogeneity uncovered by rapid freeze−quench Mössbauer spectroscopy of protein from *M. capsulatus* (Bath) (*6*) and EXAFS studies of H_{ox} from *M. trichosporium* (OB3b) hydroxylase (*17*). Scheme 1 depicts three possible structures that might be considered. Structure **1** contains a bis(μ-hydroxo)diiron(III) core and a terminal water molecule on Fe1. In structure **2** (or **4**), the proton has shifted from the terminal water to one of the bridging positions, affording a (μ-aqua)(μ-hydroxo)-diiron(III) unit. Both di(μ-hydroxo) and (μ-aqua)(μ-hydroxo) structures have been observed in the X-ray studies of H_{ox} (*12*, *13*). The third possibility (**3**) is that only one solvent-derived ligand, a hydroxo group, links the two iron atoms in addition to Glu 144, as suggested to explain the EXAFS results (*17*). These structures would be expected to have different exchange coupling constants, *J*, and zero-field splitting parameters, *D*. The bis(μ-hydroxo)diiron(III) core (**1**) should have the largest magnitude *J* and probably the lowest spread in *g* values and also $P_{1/2}$ value. Because a bridging water molecule will be easier to deprotonate than a terminal one, **1** would form preferentially at higher pH. We therefore tentatively assign H1 to this structure. Species **2**−**4** should afford a more anisotropic signal upon cryoreduction, and we suggest that H2 may correspond to one of these two alternative geometries. The relative intensity of the H2 signal depends on pH, the presence of component B, reoxidation of the MMOH/MMOB complex, and annealing of the sample at 115 K for 20 min. These observations provide indirect evidence that in fluid solution the H1 and H2 forms are in dynamic equilibrium.

Effects of Added DMSO and Alcohols. DMSO does not measurably perturb the EPR properties of Hox_{mv} reduced at 77 K, indicating that DMSO most likely does not bind directly to the diiron(III) center. This result is consistent with other observations. The crystal structure of H_{ox} from *M. capsulatus* (Bath) soaked in DMSO failed to reveal this molecule in the active site (*27*). Moreover, addition of 0.3 M DMSO to the resting H_{ox} from *M. trichosporium* OB3b had no effect on the Mössbauer spectrum of the diiron center (*15*).

Unlike DMSO, phenols apparently can coordinate directly to iron at the active site of H_{ox} (*25*). This interaction is evident in the EPR spectrum of $(H_{ox} + NO_2Ph)_{mv}$ trapped at 77 K. Two observed signals, HP1a and HP1b, are assigned to *p*-nitrophenol complexes with the H1 form (**1**) of the diiron cluster. That signal H2 remains unchanged in the mixed-valent EPR spectrum suggests that the phenol displaces the terminally coordinated water in **1**, which is not available in **2**, and provides evidence that H1 and H2 diiron(III) centers react differently toward exogenous ligands.

The significant changes in the EPR spectra of cryoreduced H_{ox} in the presence of methanol reflect perturbations of the active site local structure, suggesting that this exogenous ligand, the product of methane oxidation, binds directly to the diiron(III) center of H_{ox}. Two new EPR signals, H1M and H2M, were identified for the methanol-bound diiron center, which might arise in several ways. One likely possibility is that the terminal water molecule in **1** (Scheme 1) is displaced by methanol, the less demanding steric and hydrogen bond donor properties of which might make it better suited for such a displacement than DMSO, which apparently does not undergo such a reaction. Moreover, like the phenols, methanol can serve as both a hydrogen bond donor and a hydrogen bond acceptor and thus perturb the water structure at the active site. Such an interaction could alter the intracomplex H-bonding interactions, and possibly even the positioning of the hydroxo and aqua ligands, for example, **1** vs **2**, perturbing the EPR spectra. Another possible explanation is that two methanol molecules might be bound to the diiron(III) center. Similarities between the H1M/H1 and H2M/H2 signals suggest that species H1M and H2M derive from H1 and H2, respectively. Quantitation reveals that cryogenically reduced H_{ox} forms mixed-valent species H1 accounting for 80% of the signal, whereas the methanol-treated H_{ox} affords species less than 40% ± 15% of H1M. The ability of methanol to affect the relative amounts of cryogenerated mixed-valent hydroxylase centers supports the previous conclusion that the resting oxidized hydroxylase isomers are in dynamic equilibrium with one another in solution.

Effects of Protein B. As already mentioned, the results of EPR and CD/MCD investigations have been taken as evidence that MMOB perturbs the structure of the diiron site in mixed-valent (*28*) and fully reduced MMOH (*10*). Our results reveal, however, that complex formation between H_{ox} and MMOB does not measurably affect the H1 and H2 EPR signal line shapes and only slightly reduces the relative intensity of signal H2. We therefore conclude that MMOB complex formation induces only minor alterations in ligand binding at the dinuclear iron center of resting MMOH. For example, changes in intraligand H-bonding and ligand geometry might occur, but carboxylate shifts are less likely. Possibly MMOB binding affects the orientation of the side chain of Leu 110 (Figure 1), which adopts two conformations in crystalline MMOH and may gate the access of substrates to the active site cavity (*29*). Such a conclusion would be

qualitatively consistent with the published X-ray absorption studies on MMOH from both *M. capsulatus* (Bath) and *M. trichosporium* OB3b (*16*, *17*). For MMOH from the latter organism, a difference occurred in the distribution of long (3.4 Å) versus short (3.0 Å) Fe···Fe distance contributions to the first shell in the presence of component B (*17*).

An alteration in protein structure induced by MMOB binding would also explain its ability to facilitate binding of DMSO and glycerol to the diiron center. Complexation with MMOB dramatically perturbs the EPR spectra of cryogenically reduced MMOH in the presence of DMSO and of glycerol at high concentrations. Several distinct EPR signals may be identified in the spectrum of the irradiated H_{ox} + MMOB + DMSO system, each of which differs from the H1 and H2 signals observed in the mixed-valent spectrum of hydroxylase with DMSO present. This result in turn implies that more than one population of diiron clusters occurs in the H_{ox} + MMOB complex treated with DMSO. Like DMSO, glycerol can bind to the diiron(III) cluster of H_{ox} with MMOB present. In the presence of 50% glycerol, a new EPR signal (HB2), as well as signals H1 and H2, appears for cryogenically reduced H_{ox} complexed with MMOB. A similar EPR signal was previously reported in the EPR spectrum of the H_{ox} + MMOB complex from *M. trichosporium* OB3b in 50% glycerol solution, γ-irradiated at 77 K, but was not recognized to result from perturbation of the cluster by glycerol (*20*). Like DMSO, glycerol can bind to the diiron(III) core of H_{ox} with MMOB present. The binding of glycerol is much weaker than that of DMSO, however, because much higher concentrations of glycerol are required to detect the EPR signal.

Of perhaps greater importance is the fact that component B induces major perturbations in complexes of H_{ox} with alcohols, as shown by the EPR properties of $(H_{ox}$ + MMOB + MeOH$)_{mv}$ and $(H_{ox}$ + MMOB + PhOH$)_{mv}$. These results imply that binding of component B to H_{ox} complexed with exogenous ligand may perturb allosterically both an equilibrium between populations of the diferric clusters and the structure of the individual clusters. Such a structural change might play a role in the catalytic cycle by providing a favorable active site geometry for substrate conversion and product release.

Since MMOB can facilitate the binding of exogenous ligands to the diiron center in H_{ox}, we were especially interested to examine cryogenically reduced H_{ox} + MMOB in the presence of methane or reductase. Addition of methane under saturating concentrations had no effect on the mixed-valent spectrum of H_{ox} complexed with MMOB. This result implies either that the substrate has a low affinity for the H_{ox} + MMOB complex or that its binding in Cavity 1 is such that the spectrum remains unchanged.

The influence of MMOR on the EPR properties of the H_{ox} + MMOB complex reduced at 77 K is manifest only after annealing the sample at 115 K. This observation suggests that reductase binding perturbs in some manner the active site pocket structure, thereby influencing the relaxation mechanism of the constrained mixed-valent cluster. Possibly, like MMOB, reductase binding perturbs slightly the coordination environment of the diiron(III) cluster and these structural changes can noticeably modify reactivity of the active site as reported elsewhere (*5*, *22*, *30*).

Scheme 2

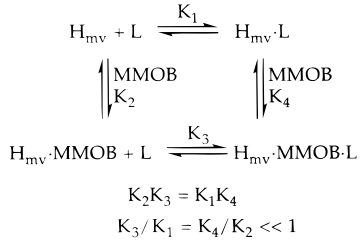

Effects of Sample Annealing. Samples of cryogenically reduced H_{ox} + MMOB + exogenous ligands annealed at room temperature correspond to H_{mv} + MMOB + L at equilibrium in solution. The results on these annealed ternary mixtures thus shed light on the ability of MMOB to affect the binding of substrates and products to H_{mv}. When the low-temperature reduced $(H_{ox} + L)_{mv}$, L = methanol or phenol, complexes are annealed at room temperature, they display the EPR spectrum of H_{mv} complexed with L. Cryogenically reduced $(H_{ox}$ + MMOB + L$)_{mv}$ (L = methanol or phenol), however, after annealing at room temperature, exhibits the EPR signals of both H_{mv} + MMOB and H_{mv} + L. These results thus indicate that L and MMOB in effect bind competitively to H_{mv} (Scheme 2). That MMOB might allosterically inhibit small molecule binding to the Fe(II)-Fe(III) center could form the mechanistic foundation for product release in MMO catalytic cycle; MMOB might be required to extrude bound product alcohols from the active site as electrons enter from the reductase. This experimentally verifiable hypothesis is currently being evaluated.

Implications for the Equilibrium Structure of the Mixed-Valent Hydroxylase. The present findings demonstrate that component B and the redox state of the diiron cluster both substantially influence the binding of exogenous ligands. Although we do not yet have direct X-ray diffraction information about H_{mv}, its altered reactivity toward small molecules compared to H_{ox} may be accounted for by a carboxylate shift similar to that observed for the fully reduced, diiron(II) form of the enzyme (*12*, *14*) (Figure 1B). ENDOR studies of H_{mv} and DMSO-treated H_{mv} from *M. capsulatus* (Bath) disclosed the presence of a hydroxo bridge and a water molecule bound to iron(II) (*8*). Possible structures for the Fe(II,III) cluster with additional carboxylate bridges are depicted in Scheme 3. These structures have vacant (**7**) or available (**5**, **6**) positions in the iron coordination spheres for the binding of exogenous ligands such as DMSO and phenols.

CONCLUSIONS

The present results, taken together with other physicochemical measurements reported for the MMO system, provide insights into the structural basis for the regulatory effect of component B. Spectroscopic data demonstrate that the interactions of MMOB with MMOH change with the oxidation state of the diiron center. This finding is consistent with alterations in redox potentials of MMOH induced by MMOB binding. The ability of component B to modify the structure and reactivity of the MMOH diiron cluster with methanol or phenol present suggests that conformational changes induced by the intercomponent interaction might play a role in the catalytic cycle, providing favorable active

Scheme 3

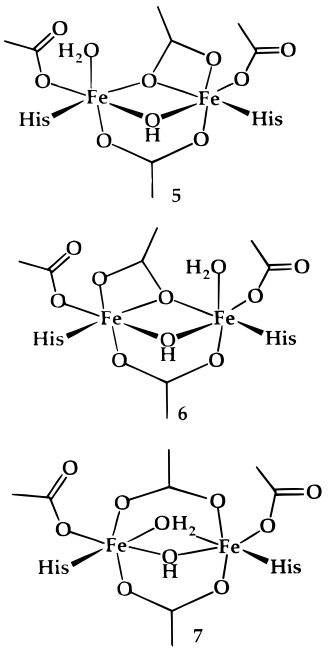

site structure for substrate conversion and product release. Opening of the leucine gate, proton-transfer reactions, and carboxylate shifting of the coordinated glutamates are suggested as specific chemical steps which could account for such behavior.

The EPR spectra of the cryoreduced samples also reveal that the resting state, oxidized hydroxylase, has at least two chemically distinct forms of diiron cluster and that their structures are different from that of the equilibrium Fe(II)-Fe(III) site. Their relative populations depend on pH, component B, and enzyme turnover. Specific proposals involving proton and carboxylate shifts at the diiron center have been put forward as a working hypothesis to explain these observations. Complex formation among MMOB, MMOR, and $MMOH_{ox}$ does not measurably affect the structure of the diiron(III) site. Cryogenic reduction in combination with EPR spectroscopy has provided information about the interaction of H_{ox} with small molecules. The diiron(III) site binds methanol and phenols, whereas DMSO and methane have no measurable effect on the EPR properties of subsequently cryoreduced samples. Addition of component B favors binding of some exogenous ligands, such as DMSO and glycerol, to the active site diiron(III) state and perturbs remarkably the structure of the diiron(III) cluster complexed with exogenous ligand (methanol, phenol). The present study also reveals different reactivity of the Fe(III,III) and Fe(II,III) sites of MMOH toward small molecule substrates. By extrapolation, the data are consistent with the possibility that substrate preferentially interacts with the fully reduced form of the hydroxylase and that component B facilitates extrusion of methanol bound to the oxidized hydroxylase upon one-electron reduction of the enzyme/product complex.

ACKNOWLEDGMENT

We are grateful to D. E. Coufal and D. A. Whittington for assistance in preparing some of the figures. We thank E. Barth (Department of Radiation Oncology, Pritzker School of Medizine, University of Chicago) for assistance with γ-irradiation.

SUPPORTING INFORMATION AVAILABLE

Four figures depicting X-band EPR spectra of cryoreduced $MMOH_{ox}$, DMSO-treated $MMOH_{mv}$, methanol-treated $MMOH_{mv}$, and $MMOH_{mv}$ in the presence of various phenols under various conditions as described in the text. This material is available free of charge via the Internet at http://pubs.acs.org.

REFERENCES

1. Dalton, H. (1980) *Advances in Applied Microbiology*, pp 71−87, Academic Press, New York.
2. Liu, K. E., and Lippard, S. J. (1995) in *Advances in Inorganic Chemistry* (Sykes, A. G., Ed.) pp 263−289, Academic Press, San Diego, CA.
3. Wallar, B. J., and Lipscomb, J. D. (1996) *Chem. Rev. 96*, 2625−2657.
4. Lund, J., and Dalton, H. (1985) *Eur. J. Biochem. 147*, 291−296.
5. Gassner, G. T., and Lippard, S. J. (to be submitted for publication).
6. Liu, K. E., Valentine, A. M., Wang, D., Huynh, B. H., Edmondson, D. E., Salifoglou, A., and Lippard, S. J. (1995) *J. Am. Chem. Soc. 117*, 10174−10185.
7. Fox, B. G., Liu, Y., Dege, J. E., and Lipscomb, J. D. (1991) *J. Biol. Chem. 266*, 540−550.
8. DeRose, V. J., Liu, K. E., Lippard, S. J., and Hoffman, B. M. (1996) *J. Am. Chem. Soc. 118*, 121−134.
9. DeWitt, J. G., Bentsen, J. G., Rosenzweig, A. C., Hedman, B., Green, J., Pilkington, S., Papaefthymiou, G. C., Dalton, H., Hodgson, K. O., and Lippard, S. J. (1991) *J. Am. Chem. Soc. 113*, 9219−9235.
10. Pulver, S. C., Froland, W. A., Lipscomb, J. D., and Solomon, E. I. (1997) *J. Am. Chem. Soc. 119*, 387−395.
11. Rosenzweig, A. C., Frederick, C. A., Lippard, S. J., and Nordlund, P. (1993) *Nature 366*, 537−543.
12. Rosenzweig, A. C., Nordlund, P., Takahara, P. M., Frederick, C. A., and Lippard, S. J. (1995) *Chem. Biol. 2*, 409−418.
13. Elango, N., Radhakrishnan, R., Froland, W. A., Wallar, B. J., Earhart, C. A., Lipscomb, J. D., and Ohlendorf, D. H. (1997) *Protein Sci. 6*, 556−558.
14. Whittington, D. A., and Lippard, S. J. (to be submitted for publication).
15. Fox, B. G., Hendrich, M. P., Surerus, K. K., Andersson, K. K., Froland, W. A., Lipscomb, J. D., and Münck, E. (1993) *J. Am. Chem. Soc. 115*, 3688−3701.
16. DeWitt, J. G., Rosenzweig, A. C., Salifoglou, A., Hedman, B., Lippard, S. J., and Hodgson, K. O. (1995) *Inorg. Chem. 35*, 2505−2515.
17. Shu, L., Liu, Y., Lipscomb, J. D., and Que, L., Jr. (1996) *J. Bioinorg. Chem. 1*, 297−304.
18. Davydov, R., Kuprin, S., Gräslund, A., and Ehrenberg, A. (1994) *J. Am. Chem. Soc. 116*, 11120−11128.
19. Davydov, R., Shalin, M., Kuprin, S., Gräslund, A., and Ehrenberg, A. (1996) *Biochemistry 35*, 5571−5576.
20. Davydov, A., Davydov, R., Gräslund, A., Lipscomb, J. D., and Andersson, K. K. (1997) *J. Biol. Chem. 272*, 7022−7026.
21. Davydov, R., Davydov, A., Ingemarsson, R., Thelander, L., Ehrenberg, A., and Gräslund, A. (1997) *Biochemistry 36*, 9093−9100.
22. Valentine, A. M., Wilkinson, B., Liu, K. E., Komar-Panicucci, S., Priestley, N. D., Williams, P. G., Morimoto, H., Floss, H. G., and Lippard, S. J. (1997) *J. Am. Chem. Soc. 119*, 1818−1827.
23. Willems, J.-P., Valentine, A. M., Gurbiel, R., Lippard, S. J., and Hoffman, B. M. (1998) *J. Am. Chem. Soc. 120*, 9410−9416.
24. Werst, M. M., Davoust, C. E., and Hoffmann, B. M. (1991) *J. Am. Chem. Soc. 113*, 1533−1538.

25. Andersson, K. K., Elgren, T. E., Que, L., Jr., and Lipscomb, J. D. (1992) *J. Am. Chem. Soc. 114*, 8711−8713.
26. Davydov, R., Menage, S., Fontecave, M., Gräslund, A., and Ehrenberg, A. (1997) *J. Biol. Inorg. Chem. 2*, 242−255.
27. Rosenzweig, A. C., Frederick, C. A., and Lippard, S. J. (1996) *Carboxylate Shifts in the Active Site of the Hydroxylase Component of Soluble Methane Monooxygenase from Methylococcus capsulatus (Bath)*, Kluwer Academic Publishers, Dordrecht, The Netherlands.
28. Froland, W. A., Andersson, K. K., Lee, S.-K., Liu, Y., and Lipscomb, J. D. (1992) *J. Biol. Chem. 267*, 17588−17597.
29. Rosenzweig, A. C., Brandstetter, H., Whittington, D. A., Nordlund, P., Lippard, S. J., and Frederick, C. A. (1997) *Proteins 29*, 141−152.
30. Liu, Y., Nesheim, J. C., Paulsen, K. E., Stankovich, M. T., and Lipscomb, J. D. (1997) *Biochemistry 36*, 5223−5233.

BI982391O